FEMS Yeast Research, 20, 2020, foaa001

https://doi.org/10.1093/femsyr/foaa001
Advance Access Publication Date: 10 January 2020
Research Article

RESEARCH ARTICLE

A subcellular proteome atlas of the yeast *Komagataella phaffii*

Minoska Valli[1,2,†], Karlheinz Grillitsch[1,†], Clemens Grünwald-Gruber[1,4,†], Nadine E. Tatto[1,2,‡], Bernhard Hrobath[5], Lisa Klug[1,3], Vasyl Ivashov[3], Sandra Hauzmayer[6,‡], Martina Koller[6,‡], Nora Tir[2], Friedrich Leisch[1,5], Brigitte Gasser[1,2], Alexandra B. Graf[1,6], Friedrich Altmann[1,4], Günther Daum[1,3] and Diethard Mattanovich[1,2,*,§]

[1]Austrian Centre of Industrial Biotechnology (ACIB), Muthgasse 11, 1190 Vienna, Austria, [2]Department of Biotechnology, BOKU-University of Natural Resources and Life Sciences, Muthgasse 18, 1190 Vienna, Austria, [3]Institute of Biochemistry, Graz University of Technology, Petersgasse 12/II, 8010, Graz, Austria, [4]Department of Chemistry, University of Natural Resources and Life Sciences, Muthgasse 18, 1190 Vienna, Austria, [5]Institute of Statistics, University of Natural Resources and Life Sciences, Peter-Jordan-Straße 82, 1190 Vienna, Austria and [6]School of Bioengineering, University of Applied Sciences FH-Campus Vienna, Muthgasse 11, 1190 Vienna, Austria

*Corresponding author: Department of Biotechnology, BOKU-University of Natural Resources and Life Sciences, Muthgasse 18, 1190 Vienna, Austria. Tel: +43 1 47654–79042; Fax: +43 1 47654–79009; E-mail: diethard.mattanovich@boku.ac.at

One sentence summary: About 2000 intracellular proteins of the methylotrophic yeast *Komagataella phaffii* were quantified and for most of them the organelle localization was attributed.

†Contributed equally.
‡Current affiliations: NET: Vienna BioCenter Core Facilities GmbH, Dr. Bohr-Gasse 3, 1030 Vienna, Austria; SH: University of Applied Arts Vienna, Oskar Kokoschka-Platz 2, 1010 Vienna, Austria; MK: AstraZeneca Österreich GmbH Landstrasser Hauptstraße 1A, 1030 Vienna, Austria.

Editor: Hyun Ah Kang

§Diethard Mattanovich, http://orcid.org/0000-0002-0907-4167

ABSTRACT

The compartmentalization of metabolic and regulatory pathways is a common pattern of living organisms. Eukaryotic cells are subdivided into several organelles enclosed by lipid membranes. Organelle proteomes define their functions. Yeasts, as simple eukaryotic single cell organisms, are valuable models for higher eukaryotes and frequently used for biotechnological applications. While the subcellular distribution of proteins is well studied in *Saccharomyces cerevisiae*, this is not the case for other yeasts like *Komagataella phaffii* (syn. *Pichia pastoris*). Different to most well-studied yeasts, *K. phaffii* can grow on methanol, which provides specific features for production of heterologous proteins and as a model for peroxisome biology. We isolated microsomes, very early Golgi, early Golgi, plasma membrane, vacuole, cytosol, peroxisomes and mitochondria of *K. phaffii* from glucose- and methanol-grown cultures, quantified their proteomes by liquid chromatography-electrospray ionization-mass spectrometry of either unlabeled or tandem mass tag-labeled samples. Classification of the proteins by

Received: 29 August 2019; **Accepted:** 9 January 2020

their relative enrichment, allowed the separation of enriched proteins from potential contaminants in all cellular compartments except the peroxisomes. We discuss differences to *S. cerevisiae*, outline organelle specific findings and the major metabolic pathways and provide an interactive map of the subcellular localization of proteins in *K. phaffii*.

Keywords: *Komagataella phaffii*; *Pichia pastoris*; yeast; protein localization; organelle; metabolic pathways

ABBREVIATIONS

ER:	endoplasmic reticulum
FC:	fold change
GO term CC:	Gene ontology term cellular component
MAM:	mitochondria-associated membranes
PC:	phosphatidylcholine
SGD:	*Saccharomyces* Genome Database
SNARE:	soluble N-ethylmaleimide-sensitive factor attachment protein receptor
PNS:	post nuclear supernatant
TMT:	tandem mass tag

INTRODUCTION

Komagataella phaffii (syn. *Pichia pastoris*) is a methylotrophic yeast frequently used as a host for the production of recombinant proteins and metabolites (for a recent review see Mattanovich, Sauer and Gasser (2017)). Apart from its application in biotechnology, it has been used as model organism to investigate secretory pathway organelles (Bevis *et al.* 2002) and synthesis and degradation of peroxisomes (Agrawal and Subramani 2016; Wang and Subramani 2017; Yamashita *et al.* 2017). For any of these applications it is essential to know the intracellular localization of as many cellular proteins as possible. Intracellular targeting of yeast proteins is usually deduced from computational predictions (https://wolfpsort.hgc.jp/; http://www.cbs.dtu.dk/services/TargetP/; http://mendel.imp.ac.at/pts1/) or from the respective *Saccharomyces cerevisiae* homologs. Huh *et al.* (2003) have visualized the localization of 75% of the *S. cerevisiae* proteome by a GFP-tagged library. Wiederhold *et al.* (2010) have integrated the data of 18 subcellular proteomics studies on *S. cerevisiae*, providing information on 61% of the predicted yeast proteome. Beside these 'global' protein localization studies, numerous data on localization of individual yeast proteins have been published and feed the Gene Ontology term Cellular Component (GO term CC) of the *Saccharomyces* Genome Database (SGD) (https://www.yeastgenome.org/). However, when drawing comparative conclusions, one must be aware of the wide phylogenetic distance of *K. phaffii* to *S. cerevisiae* (Shen *et al.* 2018). During their evolution, proteins may have adopted novel functions or different intracellular localization, as we have shown recently for homologs of the pentose phosphate pathway (PPP) enzymes in *K. phaffii* (Russmayer *et al.* 2015). Therefore, an independent experimental determination of intracellular protein localization is indispensable for detailed knowledge of cell biology and physiology of this yeast.

To understand and model metabolic pathways, their compartmentalization is a critical issue. Already the first genome scale yeast metabolic model considered compartmentalization of its reactions (Förster *et al.* 2003) and was further updated by community efforts to the current version Yeast8 (Lu *et al.* 2019). While most pathways of the eukaryotic primary metabolism have a canonical localization in the cytosol, mitochondria or peroxisomes, some reactions of amino acid or nucleotide synthesis are differently localized between the cytosol and the mitochondria in different yeasts (Nagy, Lacroute and Thomas 1992; Förster *et al.* 2014). Characterization of the secretory pathway also requires knowledge in the intracellular localization. Although the core functions are highly conserved among yeasts, accessory proteins like J-proteins, members of the protein disulfide isomerase (PDI) family and enzymes for N- and O-glycan modification show diversities (Delic *et al.* 2013). Similarly, although vacuolar protein sorting pathways are highly conserved, there are differences in components of the autophagy pathway and the function of subunits of the Golgi-to-vacuole transport machinery is not well characterized for non-*Saccharomyces* yeasts (Tamura, Oku and Sakai 2010; Polupanov, Nazarko and Sibirny 2011; Marsalek *et al.* 2017).

Gene fusions with a fluorescent protein enable the creation of a genome scale library for visual inspection by live cell microscopy but bear the risk to distort the localization of individual proteins in an unpredictable way. Subcellular fractionation on a density gradient, combined with mass spectrometry and computational prediction methods (hyperplexed localization of organelle proteins by isotope tagging (hyperLOPIT) (Christoforou *et al.* 2016; Nightingale *et al.* 2019) allows to get the subcellular proteome in a single experiment but the classification attributes the localization of proteins to only one subcellular location. Organelle fractionations, on the other hand, are prone to carry over contaminations, as evaluated in detail by Wiederhold *et al.* (2010), but may be considered as a more unbiased biochemical method to identify the localization of individual proteins. Both fluorescent protein fusions and mass spectrometry-based proteomics suffer of a bias toward more abundant proteins, which is inevitably linked to the sensitivity of the detection method. While methods for yeast organelle fractionation have been well established for *S. cerevisiae* (Wiederhold *et al.* 2010), these protocols need to be adapted for other yeasts. In the last decade, methods for the isolation of peroxisomes, mitochondria, lipid droplets, microsomes and plasma membrane of *K. phaffii* have been developed (Wriessnegger *et al.* 2007; Wriessnegger *et al.* 2009; Ivashov *et al.* 2013a; Grillitsch *et al.* 2014; Klug *et al.* 2014). These protocols, together with the separation of the Golgi apparatus and the vacuole, provide an ideal basis for organelle specific fractionation of *K. phaffii* cells for mass spectrometry-based proteome identification and quantification.

In this work, we focused on two aspects: the proteome of each organelle, looking for proteins required for organization and function of the organelle and the primary metabolic pathways, looking for enzymes involved in carbon metabolism, amino acid pathways, nucleotide synthesis, beta-oxidation and lipid metabolism. We focused on localization patterns different from the *S. cerevisiae* homologs, source specific localizations and provide an online tool to browse the information on subcellular protein localization.

EXPERIMENTAL PROCEDURES

Strains and culture conditions

Komagataella phaffii CBS7435 was pre-cultivated at 25°C for 48 h in YPD (1% yeast extract, 2% peptone and 2% glucose), cultivated with starting OD_{600} of 0.1 in YPD and 0.15 in YPM (1% yeast extract, 2% peptone and 1% methanol) and harvested after 25 and 28 h, respectively.

Isolation of cellular compartments and quality control of the organelle specific fractions

Komagataella phaffii subcellular fractions were generated with slight modifications of published procedures (Ohsumi and Anraku 1981; Wriessnegger *et al.* 2007; Wiederhold *et al.* 2009; Wriessnegger *et al.* 2009; Grillitsch *et al.* 2014; Klug *et al.* 2014). Golgi and vacuole fraction isolations were first established with strains expressing GFP fusions of specific markers: v-SNARE Sed5 and t-SNARE syntaxin Gos1 for the Golgi fractions and Vac8 for the vacuole (Table S1 and Fig. S1, Supporting Information File 1). Proteins of all isolated fractions were precipitated with trichloroacetic acid, quantified with BSA (Lowry *et al.* 1951) and analyzed by SDS-PAGE (Laemmli 1970) and immunoblot analysis (Haid and Suissa 1983). Fraction purity was tested by Western Blot using in-house raised antibodies against *S. cerevisiae* markers (mitochondrial porin Por1, plasma membrane ATPase Pma1 and glucanosyltransferase Gas1 and cytosolic glyceraldehyde-3-phosphate-dehydrogenase GAPDH) or against the *K. phaffii* 75 kDa ER marker protein and antisera against peroxisomal membrane protein Pex3 and integral Golgi protein Emp47, provided by R. Erdmann and H. Riezman, respectively (Fig. S2 and S3, Supporting Information File 1).

Experimental design and statistical rationale

Eight subcellular fractions (microsomes, very early Golgi, early Golgi, plasma membrane, vacuole, peroxisomes, cytosol and mitochondria) and PNS were isolated from glucose- and methanol-grown cells. Purity and enrichment of the fractions were confirmed by specific markers (see above). Two biological and two technical replicates were analyzed.

MS analyses

Pellets of the isolated fractions and PNS were reconstituted in 2% SDS, 30 mM tris(2-carboxyethyl) phosphine (TCEP), 200 mM triethylammonium bicarbonate buffer (TEAB buffer) and incubated at 95°C for 5 min. The supernatants obtained after centrifugation (13 000 × *g* for 5 min), were treated for reduction of disulfide bonds, carbamidomethylation and MeOH/chloroform precipitation (Russmayer *et al.* 2015). Tryptic digestion (sequencing grade modified trypsin, Promega) was performed overnight in 100 mM TEAB buffer at 37°C. The peptide mixture was either directly injected in a nano LC-ESI-MS system or tandem mass tags (TMT) labeled (Pichler *et al.* 2010). The TMT-labeled samples were combined (each subcellular fraction with the homogenate to allow the comparison among compartments: for details see Supporting Information File 2) and fractionated by reversed phase chromatography at pH 10 with a Dionex Ultimate 3000 system equipped with a Waters XBridge BEH130 C18 3.5 µm 300 × 150 NanoEase column. A gradient of 12.5% to 80% acetonitrile (100%) in ammonium formate buffer (200 mM pH 10) over 60 min was applied. Fractions were collected every 200 seconds and 12 fractions were selected for nanoLC-MS measurement (fractions 1 to 3 were discarded and the fractions 4 to 6 and 17 + 18 were pooled).

Samples were analyzed with a nano LC system (Dionex Ultimate 3000) with a Thermo Acclaim PepMap RSLC C18 column (2 µm, 0.075 mm ID, 250 mm length), combined with a Thermo Acclaim PepMap µ-Precolumn (C18 0.300 × 5mm). A gradient of 5% to 90% solvent B (80% acetonitrile + 20% 0.1% formic acid) in solvent A (0.1% formic acid in water) was applied to unlabeled and TMT-labeled fractions over 180 min and 90 min, respectively. Detection was performed with a QTOF MS (Bruker maXis 4 G ETD) with the captive spray ion source in positive ion, DDA mode (switching to MS/MS mode for eluting peaks) using a nanobooster. MS-scans were recorded (range: 150–2200 Da) and the eight highest peaks were selected for fragmentation. Instrument calibration was performed using ESI calibration mixture (Agilent). DataAnalysis 4.0 was used to process the data and create xlm or mgf files suitable to perform MS/MS ion search with ProteinScape (MASCOT embedded, Version 2.3.02). Protein identification was done using an internal protein database of 5339 IDs (Supporting Information File 3), obtained from the manual curation of all *K. phaffii* protein IDs available in Uniprot by 2014 (https://www.uniprot.org/) which excluded duplicates and wrongly predicted sequences. Fixed modifications (carbamidomethyl: C, TMT 6 plex (only for labeled samples): K and N-term), variable modifications (oxidation: M) and one missed cleavage were permitted. Measurement errors were set to 0.05 Da for fragment ions and +/− 7 ppm for parent ions mass. Only proteins identified from at least two peptides, each with a MASCOT score above 30 (FDR < 1%), were further considered (All identified proteins, with respective sequence coverage are shown in Supporting Information Files 2 and 4). In case of protein isoforms or identical proteins, the values were attributed to all proteins.

MS data processing

In the unlabeled experiment, the biological replicates were processed independently. We accepted proteins found in both technical replicates of each biological replicate and calculated the average of the MASCOT scores. In the TMT-labeled experiments, the fold change (FC) of the signal of each protein in a specific fraction against the PNS was normalized by the amounts of protein present in the analyzed samples (Supporting Information File 5). Only proteins found in all four replicates were accepted (identified by more than one peptide in all four replicates or identified by more than one peptide in three replicates but only if the sum of the peptides from all replicates was higher than eight), as well as proteins found only in three replicates but always with more than one peptide. For all proteins fulfilling those criteria, we calculated the mean of the FCs and the corresponding $\log_2$FC.

Analysis procedure to define enrichment cut-off

Based on the frequency distribution of the $\log_2$FC value of the quantified proteins (Fig. 2A), estimation of a mixture model was the first part of the analysis (Fig. 1, left part). We used a model with two Gaussian components, each with an own mean and variance. Estimation was done with the statistical software R (https://www.R-project.org/) (R Core Team 2017) and the R-package 'Mclust' (Fraley *et al.* 2012), which uses an expectation-maximization (EM) algorithm (Fraley and Raftery 2002; Fraley

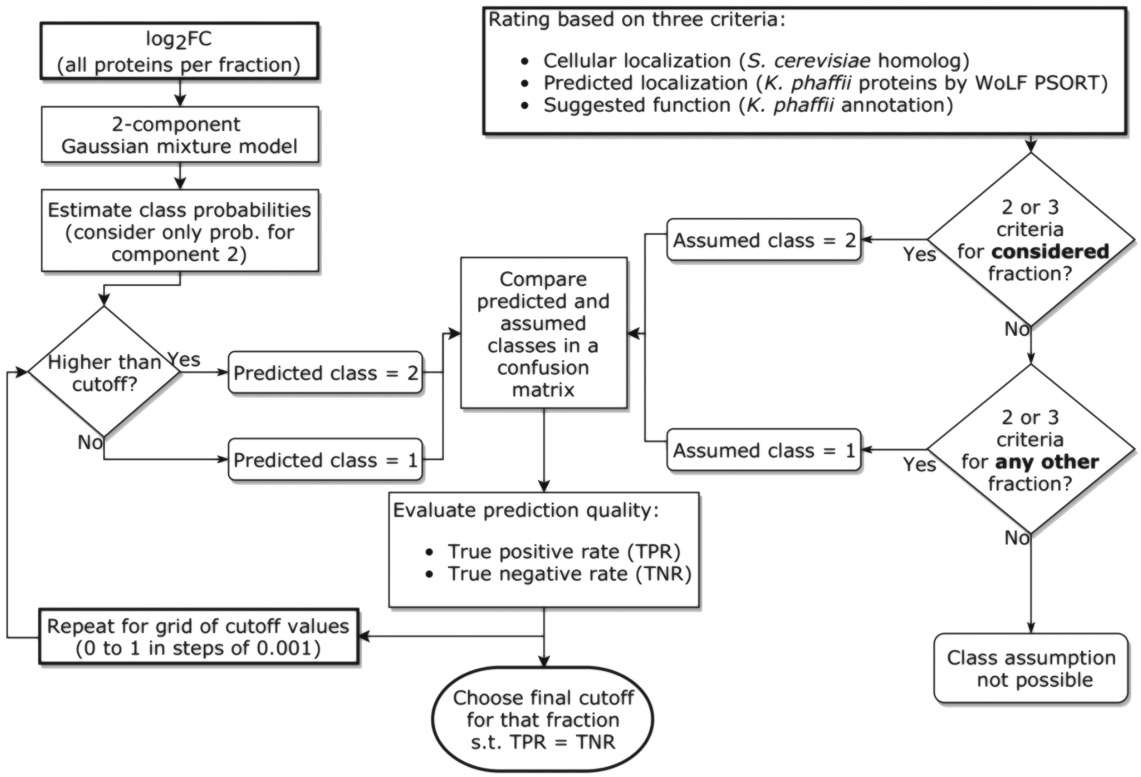

Figure 1. Analysis workflow for definition of enrichment cut-offs. The two uppermost boxes denote the two types of input data, which were used via this pathway for cut-off definition: frequency distribution of the log_2FC values and protein expectation based on a rating system. The central part shows the comparison of predicted and assumed classes for the definition of the enrichment cut-offs, which is the endpoint of this analysis path. The analysis was applied separately to data from each fraction from glucose- and methanol-grown cells.

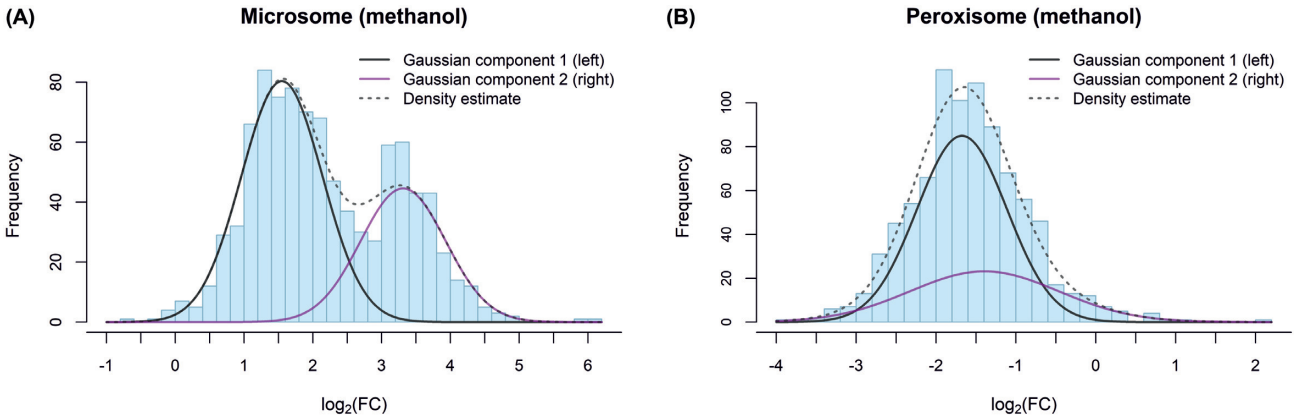

Figure 2. Examples of frequency distributions of the quantified proteins. Blue bars denote the frequency of proteins within specific intervals of log_2FC values. The dotted black line (density estimate) represents the estimated mixture distribution based on the two Gaussian components 1 and 2, shown in black and purple, respectively. **(A)**, Microsomes from methanol-grown cells with two populations. **(B)**, Peroxisomes from methanol-grown cells with a single population. All other distributions are shown in Fig. S4 and S5 (Supporting Information File 1).

et al. 2012) for parameter estimation. We call the component with the lower estimated mean 'component 1' and the one with the higher estimated mean 'component 2'. The corresponding classes are called 'class 1' and 'class 2'. The estimation procedure gives probabilities that a protein belongs to these classes. As the probabilities sum up to 1, we only used the estimated probability that a data point belongs to class 2 to define cut-off values for class prediction.

The second part of the workflow concerns the definition of expected proteins in a certain fraction (Fig. 1, right part). This was done with a rating system based on three criteria: the cellular localization of the *S. cerevisiae* homolog based on the manually curated GO term CC (https://www.yeastgenome.org/), the predicted localization of *K. phaffii* proteins suggested by WoLF PSORT (https://wolfpsort.hgc.jp/) and the function suggested by the gene/protein description of the *K. phaffii* annotation

(http://www.pichiagenome.org). For each protein and each fraction, the number of fulfilled criteria was summed up and used as final rating (Supporting Information File 6). If the final rating was 2 or 3, the protein was considered as expected in a fraction. Because of the difficult prediction of vacuolar localization, a maximal rating of 2 was only possible for the vacuole. Moreover, a correction on the expectation of proteins with Golgi, plasma membrane or vacuole, as final localization, was introduced to avoid them to be considered as contaminants in the fractions of the transit organelles microsomes, very early and early Golgi. The information about the expected proteins for the specific fractions or for any other fraction were used to derive the 'assumed' classes 2 and 1 (Fig. 1).

Finally, based on the comparison of the predicted and assumed classes, two quality measures were calculated. These are referred to as true positive rate (TPR) and true negative rate (TNR) (Powers 2011) and should ideally both be high. We evaluated the predictions based on a grid of cut-off values and chose for each fraction the final cut-off when both quality measures were equal (Fig. 1, central part).

As the protein distribution in the peroxisomes did not separate well into two components (Fig. 2B), we could not exclude proteins as probably false positives as for the other fractions and therefore excluded the 5% of data with the lowest $\log_2$FC value and considered the remaining proteins as enriched in the peroxisomes. The low threshold was chosen to keep the number of false negatives down.

Once a cut-off for each data set had been defined, we could distinguish between proteins above the cut-off considered as 'enriched' and proteins below the cut-off, considered as 'only quantified' in a certain cellular compartment (Supporting Information File 6).

Design of the graphical web-based proteome atlas

The graphical web based representation of the *K. phaffii* proteome was developed by using HTML5 (https://www.w3.org/TR/html5/), CSS3 (https://www.w3.org/TR/css-2017) and JavaScript (https://developer.mozilla.org/en-US/docs/Learn/JavaScript). A scalable vector graphic file SVG (https://www.w3.org/TR/SVG2/) was used as a basis for the display of the yeast cell and its cellular compartments. The data were dynamically loaded and displayed from a JavaScript Object Notation (JSON) (http://json.org/) file using D3.js (https://d3js.org/). For autocompletion JQuery (https://jquery.com/) libraries (jquery-1.10.2.js, jquery-ui.css, jquery-ui.js) were used. Tooltips were created and colors were changed with D3.js (d3.v3.min.js, d3.tip.v0.6.3.js, queue.v1.min.js, topojson.v1.min.js) (http://labratrevenge.com/d3-tip/, https://(?PMU?)github.com/Caged/d3-tip). Google font Raleway or Lato (https://fonts.googleapis.com/css?family=Lato, https://fonts.(?PMU?)googleapis.com/css?family=Raleway) was used. BootstrapCDN (bootstrap.min.js v3.3.6, bootstrap.min.css v3.3.6) (https://maxcdn.bootstrapcdn.com/bootstrap/3.3.6/js/bootstrap.min.js, https://maxcdn.bootstrapcdn.com/bootstrap/3.3.6/css/bootstrap.min.css) was used for responsive design and component creation in the document object model (DOM). Data uploaded on the interactive map were normalized to directly compare enrichment of a protein in different cellular compartments. For each compartment we considered the value c as the arithmetic mean between the highest observed $\log_2$FC with predicted class 1 and the lowest observed $\log_2$FC with predicted class 2. See equation 1 for normalization of $\log_2$FC values below *c* and equation 2 for values above *c*.

$$x'_i = (x_i - c)/(c - min\ (x)) \text{ if } x_i \leq c \quad (1)$$

$$x'_i = (x_i - c)/(max\ (x) - c) \text{ if } x_i > c \quad (2)$$

By this normalization, for each cellular compartment the $\log_2$FC values at the cut-off were set to zero, the smallest and largest values were set to -1 and 1, respectively (Supporting Information File 6).

RESULTS

Definition of enrichment of *K. phaffii* proteins in each fraction

Microsomes (vesicular structures that originate during the isolation of the ER), very early and early Golgi, plasma membrane, vacuole, peroxisomes, cytosol and mitochondria were isolated from *K. phaffii* cultivated in glucose or methanol until mid/late exponential phase. 1999 *K. phaffii* proteins were quantified by comparative proteomics. The dual distribution of the protein frequency observed in all fractions except the peroxisomes, was modeled with two Gaussian components, whereas the peroxisomes were modeled with one single component (Fig. 2; Fig. S4 and S5, Supporting Information for all distributions). As the enrichment of a certain protein in a fraction cannot be easily calculated due to the different volumes the specific organelles occupy in the cells, we used an approach based on expected protein localization. Indeed, proteins expected in the specific fraction fall into component 2 and proteins only expected in the other fractions ('contaminants') fall into component 1 (Fig. 3A; Fig. S6 and S7, Supporting Information left side for all distributions). Statistical data processing allowed the definition of cut-offs and of 'correctly predicted class 2' proteins, further considered as 'enriched' (Fig. 3B and Fig. S6 and S7, Supporting Information right side for all distributions).

Of the 1999 quantified proteins, 1853 were classified as enriched in at least one fraction while the rest was below the cut-off. Indeed, 1408 proteins were enriched in fractions derived from both glucose- and methanol- grown cells, while 307 and 138 proteins were enriched in either glucose- or methanol-grown samples, respectively. A total of 61 proteins were additionally detected in unlabeled samples, but not quantified in TMT-labeled samples, probably due to their low concentration in the PNS. Except for the very early Golgi, more proteins were quantified in fractions derived from glucose-grown cells compared to the ones from methanol (Fig. 4 and Supporting Information File 7 with the proteome of each of the studied organelles listed separately). The lower number of proteins quantified in methanol-derived fractions might be due to the low abundance of some proteins in the PNS, in the fractions or in both. The high number of proteins enriched in the peroxisomes is only a consequence of the single component distribution and the different cut-off procedure used, that did not allow the separation of potential contaminants. In the following data discussion, the expression 'protein found' will always refer to 'protein found enriched'.

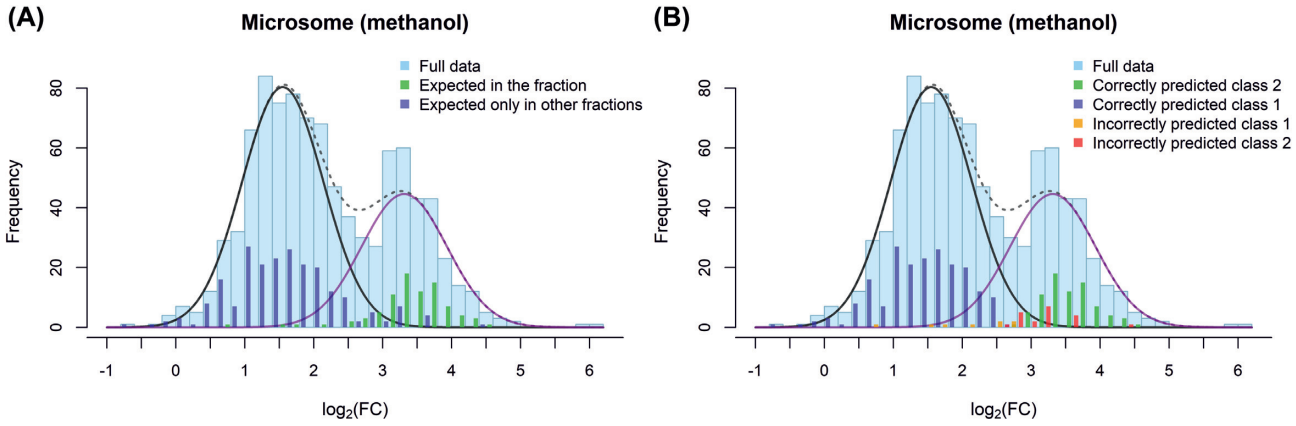

Figure 3. Example of frequency distribution of the expected proteins (in the specific fraction or only in other fractions) and the predicted proteins (in class 1 or class 2). As in Fig. 2, the light blue bars denote the frequency of proteins within specific intervals of log_2FC values, the dotted black line (density estimate) represents the estimated mixture distribution based on the two Gaussian components 1 and 2, shown in black and purple, respectively. **(A)**, Proteins expected in the specific fraction according to the rating are shown in green, whereas proteins expected only in other fractions are in blue. **(B)**, With the definition of the cut-off, proteins were further classified. Proteins expected in the fraction were classified into 'correctly predicted class 2' (green) and 'incorrectly predicted class 1' (orange), whereas the proteins expected only in other fractions were further classified into 'correctly predicted class 1' (blue) and 'incorrectly predicted class 2' (red). All other distributions are shown in Figs S6 and S7 (Supporting Information File 1).

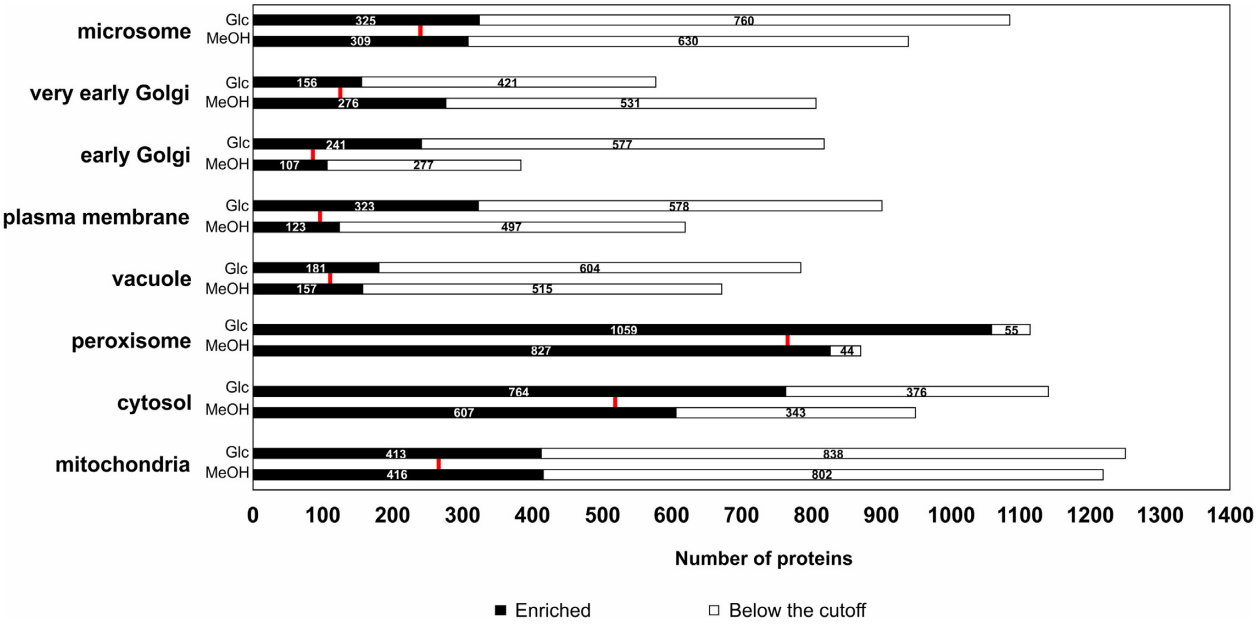

Figure 4. Overview of the numbers of quantified proteins in the respective fractions. For each fraction, the number of proteins found enriched (in black) and below the cut-off (in white) from glucose-grown cells (Glc) and methanol-grown cells (MeOH) is reported. The red dotted lines, which connect the two bars of each organelle, indicate the number of proteins enriched on both growth conditions tested. Note that the higher number of enriched proteins in the peroxisomes is a consequence of the different cut-off method used to analyze this fraction.

Comparison to expected localization of *S. cerevisiae* homologs

Differences in the localization of *K. phaffii* and *S. cerevisiae* homologs were investigated considering all *K. phaffii* proteins enriched in at least one of the fractions isolated from glucose-grown cells, which have an *S. cerevisiae* homolog with manually curated GO term CC assigned. 236 *K. phaffii* proteins were found to be enriched in an organelle different from the one described for *the S. cerevisiae* homolog (Supporting Information File 8). One third of these proteins, however, should not be considered to have a different localization. A total of 26 of them are localized in the later secretory pathway or the plasma membrane and expected to be enriched also in microsomes and/or Golgi as they transit through those organelles to reach the final destination. For 51 *S. cerevisiae* proteins a different localization is suggested by their function in the gene/protein description or by the GO term CC from high-throughput data, fitting to the *K. phaffii* localization. Of the remaining *K. phaffii* proteins, 29 were expected to have a different localization to *S. cerevisiae* based on the different predicted localization, which underlines a functional difference between the two yeasts. Fig. 5 shows in which organelles the 236 proteins were found and if their different localization can be explained based on the criteria described above.

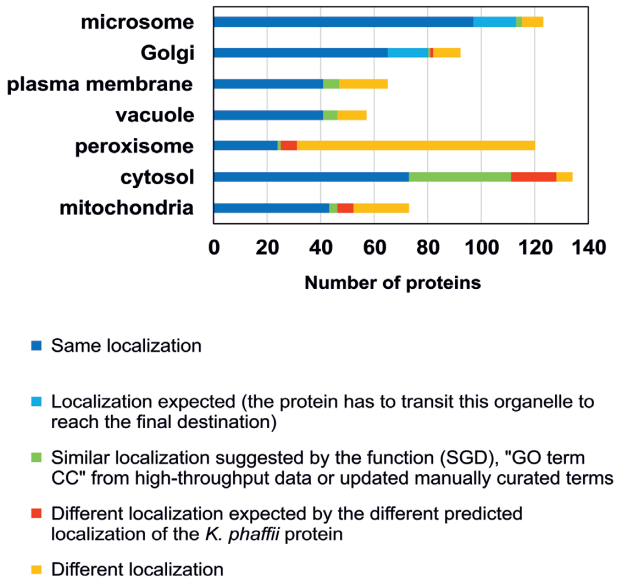

Figure 5. Comparison of protein localization between *K. phaffii* and *S. cerevisiae*. The numbers refer to *K. phaffii* proteins enriched in fractions isolated from glucose-grown cells, which have an *S. cerevisiae* homolog with manually curated GO term 'Cellular Compartment' assigned. There are proteins with the same localization (blue bars), proteins expected to be found in organelles like microsome and Golgi because they have to transit through those organelles to reach the final destination (light blue bars), proteins with a suggested same localization based on their function/role in *S. cerevisiae* defined by the description and/or the assigned GO term CC from high throughput data (green bars), proteins with a different localization explained by their different predicted localization (red bars) and proteins with a different localization not explained by the predicted localization or by available information in the literature (orange bars).

Main features of the organelle specific proteomes

Microsomes

The microsome proteome contains ER proteins, proteins required for inter-organelle ER communication and proteins that need to pass through the ER to reach their final localization. A dual localization, in microsome and very early Golgi, was found in fractions from methanol-grown cells for chaperones, enzymes of ER glycosylation and lipid metabolism, the glycosylphosphatidylinositol transamidase complex, the translocon pore, and proteins related to beta-1,6-glucan synthesis. Early Golgi enzymes must be recycled through the ER (Dean 1999) but due to the higher specific protein synthesis rate and total protein content in *K. phaffii* cultivated on methanol (Russmayer *et al.* 2015), the higher protein transit between ER and Golgi might delay this recycling. The better separation of the two protein populations in very early Golgi from methanol-grown cells (see corresponding distribution in Supplementary Fig. S4 and S5), further supports the biological meaning of the dual localization. Many unknown proteins were found among the most enriched proteins, and one is the most enriched in microsomes from methanol-grown cells. Highly abundant in microsomes isolated from both growth conditions are the ER proteins Stt3, Ero1, Bud6 and the unknown protein encoded by PP7435_Chr3–1161.

Golgi

The Golgi proteome is discussed here considering both very early and early Golgi fractions. Similarly to the microsome, we found many transporters that have to be processed along the secretory route, but surprisingly, some were never quantified in the organelle of destination. Due to the functional connection between ER and Golgi, proteins found in the Golgi were in most of the cases also found in the microsomes (Karhinen and Makarow 2004). Highly abundant in all Golgi fractions isolated from both growth conditions are the mannosyltransferases PpBmt2, PpBmt3 and Ktr1.

Protein glycosylation

The core pathways of N- and O-glycosylation are nearly identical to *S. cerevisiae* (Puxbaum, Mattanovich and Gasser 2015), but glycan modification by addition of mannose residues differs markedly as *K. phaffii* glycans are typically much shorter and less branched (Dean 1999; Hamilton *et al.* 2003; Vervecken *et al.* 2004; Maccani *et al.* 2014). However, only few of the involved enzymes were quantified in this study. Synthesis of dolichyl-linked mannose and glucose, to be transferred to N- and O-glycans in the ER, takes place at the cytosolic side, but similarly to *S. cerevisiae* the respective transferases Alg5 and Dpm1 were found in the microsome fraction. Most members of the oligosaccharyl transferase (OST) complex, the O-mannosyl transferase (PMT) subunits and the enzymes for initial glycan modification and of the calnexin cycle, were found in the microsomes, and the mannosyl transferases for elongation of glycans in the Golgi. As expected, some of the enzymes for the synthesis of activated sugars (UDP-glucose, GDP-mannose and UDP-N-acetylglucosamine) were found in the cytosol and the GDP-mannose transporter Vrg4, which provides the substrate for glycan mannosylation, was found in the Golgi.

Plasma membrane

The plasma membrane proteome shows a significantly higher enrichment of plasma membrane transporters in methanol-grown cells. Although *K. phaffii* is enzymatically well equipped with the methanol utilization pathway when methanol is the carbon source, apparently glucose is the favored carbon source as the cells eagerly express and implement high-affinity glucose transporters in the plasma membrane also when a different carbon source is used. This suggests that on a less favorable carbon source the cells get prepared for the uptake of other nutrients. Highly abundant in plasma membrane isolated from both growth conditions, are the plasma membrane transporters Ctr1, Snq2, Pdr5, Pma1 and Tpo1, the actin related proteins Bud6 and Prk1, the elongator complex subunit Elp4, and the protein Pum7 whose function is still unknown.

Vacuole

Few unexpected results came up in the vacuolar proteome, mainly related to the vacuolar iron metabolism. Mitochondrial localization was found for the iron oxidase Fet5 (Urbanowski and Piper 1999), in agreement with a predicted mitochondrial localization but differently from the *S. cerevisiae* homolog which forms a complex with Fth1 on the vacuole surface. Other proteins involved in transport or metabolism of iron and iron-related compounds were found, but their involvement in sequestration and mobilization of intravacuolar iron is unclear. In contrast to the luminal vacuolar proteome of *S. cerevisiae* (Sarry *et al.* 2007) and despite the similar growth conditions for the glucose-grown cells, we found only a low number of cargo proteins, targeted to the vacuole for degradation, processing or salvage. Enzymes for methanol utilization were found in the vacuole cargo, further suggesting their synthesis and degradation in glucose-grown cells. The vacuolar membrane proteome (Wiederhold *et al.* 2009) and luminal proteome (Sarry *et al.* 2007) have been studied in *S. cerevisiae*. There is a large

overlap between the vacuolar membrane proteome of *S. cerevisiae* (Wiederhold *et al.* 2009) and the *K. phaffii* vacuole proteome presented here. Most notably, 17 of the 30 uncharacterized *S. cerevisiae* proteins detected by Wiederhold *et al.* (2009) (24 thereof with homologs in *K. phaffii*), were confirmed to be vacuolar resident proteins also for *K. phaffii*. Many unknown proteins are found in the vacuole among the most enriched proteins. Notably, 13 vacuolar proteins were shared between the 40 most enriched proteins in the vacuole isolated from both glucose- and methanol-grown cells. This is the highest consensus among all tested fractions and indicates an especially high quality of vacuolar preparations.

Peroxisomes

More peroxisomal proteins were found in the peroxisomes from methanol-grown cells. This was expected because peroxisomes are much more abundant if methanol is the carbon source (Johnson *et al.* 1999). We found the dynamin-like proteins Dnm1 and Vps1, key players of peroxisome fission in *Ogataea polymorpha* and *S. cerevisiae*, respectively, suggesting the involvement of both proteins in peroxisome fission of *K. phaffii*. The finding of more actin related protein compared to the other fractions, suggest a higher requirement of actin structures for the movement of peroxisomes. Differently, the finding of most tubulin related proteins should be only a consequence of the close proximity of peroxisome to microtubules as shown in *S. cerevisiae* (Just and Peranen 2016), because movement of peroxisomes along microtubules is only known for mammalian cells (Schollenberger *et al.* 2010). The putative Pex26 encoded by PP7435_chr4–0482, the fatty-acyl coenzyme A oxidase Pox1, a member of the ER membrane complex Emc1 and the unknown protein encoded by PP7435_chr1–2500 were highly abundant in peroxisomes isolated from both growth conditions. Half of the proteins of the minimal *S. cerevisiae* peroxisome proteome and of the ancestor eukaryotic peroxisome proteome predicted by Gabaldón *et al.* (2006) were found, while the rest was never quantified. Although only part of predicted and expected peroxisomal proteins were quantified, their unique localization in the peroxisome was confirmed.

Cytosol

The proteome of the cytosol shows a high consensus: approximately half of the proteins quantified in cytosol were enriched in fractions from both carbon sources, compared to 20% of consensus found in other fractions, excluding the peroxisomes. The finding of many vacuolar and plasma membrane proteins (mainly transporters) in the cytosol supports the hypothesis that these proteins remain in intermediate organelles on their passage. Some were not quantified at their predicted destination, probably because of degradation or delay due to regulatory mechanisms.

Mitochondria

In the mitochondrial proteome we found enzymes of mitochondrial metabolic pathways like the TCA cycle, amino acid metabolism, folate synthesis and most of the subunits of the five complexes of the respiratory chain. Noteworthy, in contrast to *S. cerevisiae*, *K. phaffii* contains also the respiratory complex I (Bridges, Fearnley and Hirst 2010), bypassed in *S. cerevisiae* by three NADH dehydrogenases present at both sides of the inner mitochondrial membrane. *K. phaffii* contains only two NADH dehydrogenases but only Nde1 was quantified, in agreement with the higher transcript level of *NDE1* compared to *NDE2* in our previous microarray experiments (Rebnegger *et al.* 2014). Rebnegger *et al.* (2014) show that Nde2 and all proteins of the complex I are upregulated at higher growth rate whereas Nde1 is upregulated at low growth rate, suggesting that Nde1 (PP7435_Chr1–1084) is actually the internal NADH dehydrogenase Ndi1 whereas Nde2 (PP7435_Chr3–0399) is the unique external NADH dehydrogenase. Endosomal and plasma membrane proteins were found probably due to the intensive communication of mitochondria with other organelles (Murley and Nunnari 2016) while the finding of proteins both in mitochondria and peroxisome, might only be consequence of their vicinity (Cohen *et al.* 2014). Proteins part of the mitochondria-associated membrane (MAM) fraction described for *S. cerevisiae* (Gaigg *et al.* 1995), might also exist in *K. phaffii*. Many unknown proteins are found in the mitochondria among the most enriched proteins, with one being the most enriched protein from methanol-grown cells.

Enzymes of primary metabolic pathways

The metabolic pathways of *K. phaffii* have been well annotated during efforts to annotate the genome, and to develop and refine metabolic models (for recent updates see Valli *et al.* (2016) and Tomas-Gamisans, Ferrer and Albiol (2018)). Correct computational simulation needs to know the existence or absence of any specific reaction as well as their localization, which are mainly inferred from knowledge on *S. cerevisiae* but prone to error if the localization is different in *K. phaffii*. In the following, the main primary metabolic pathways are discussed.

Carbon metabolism

Glucose uptake In the plasma membrane of glucose-grown cells only the low affinity transporter Hxt1 was found, while the high-affinity transporters Gth1 might not be expressed because of the high-glucose concentrations (Prielhofer *et al.* 2013). However, both transporters were found in the plasma membrane from methanol-grown cells (see plasma membrane discussion).

Glycolysis All glycolytic enzymes were found as expected in the cytosol of both glucose- and methanol-grown cells. No association of glycolytic enzymes to the mitochondrial surface was observed, in contrast to what was shown in *S. cerevisiae* (Brandina *et al.* 2006) and in *Arabidopsis thaliana* (Wojtera-Kwiczor *et al.* 2013) and suggested by SGD GO terms.

PPP All PPP enzymes except Rki1–1 were found in the cytosol of glucose-grown cells, plus in some more compartments. Most cytosolic PPP enzymes were found in the cytosol on methanol, while the methanol induced isoenzymes identified by Russmayer *et al.* (2015) were in the peroxisomes.

TCA cycle Prior to entering the TCA cycle, pyruvate is transported into mitochondria by a mitochondrial pyruvate carrier, a heterodimeric complex of the inner membrane recently identified by Herzig *et al.* (2012). In *S. cerevisiae*, this carrier consists of Mpc1 and Mpc2 during fermentative growth or Mpc1 and Mpc3 during respiratory growth, but *K. phaffii* has only the genes *MPC1* and *MPC3*. Mpc1 was found in the mitochondria in both tested growth conditions, while Mpc3 was found in the mitochondria only below the cut-off. Beginning with the pyruvate dehydrogenase complex, most TCA cycle enzymes were found in the mitochondria in both conditions, with the exception of Cit1, Aco1, Idh1 and Idh2, found in the mitochondria on methanol, but below the cut-off on glucose.

All TCA cycle enzymes found in the mitochondria were also found in the peroxisomes. Whether this is due to dual localization will need further investigations. Due to the absence of several peroxisomal paralogs (first of all, peroxisomal citrate synthase Cit2), the dual localization might feed the peroxisomal and cytosolic pools of intermediary metabolites. The *S. cerevisiae* genome encodes three malate dehydrogenases: the mitochondrial Mdh1, cytosolic Mdh2 and peroxisomal Mdh3. Differently, In *K. phaffii* there are only two malate dehydrogenases, Mdh1 found in the peroxisomes on glucose (and below the cut-off in the mitochondria) and Mdh3 in the cytosol in both cultures, but no Mdh with mitochondrial localization. The present data suggest that different to *S. cerevisiae* the entire TCA cycle (and not only the upper part feeding the glyoxylate cycle) might be active in peroxisomes in *K. phaffii*. Alternatively, malate can be decarboxylated to pyruvate by the mitochondrial malic enzyme Mae1, which fills the pyruvate pool for mitochondrial amino acid synthesis (Boles, de Jong-Gubbels and Pronk 1998). In *K. phaffii*, however, Mae1 was only found in the peroxisomes and cytosol, indicating a different role or localization of the respective amino acid synthesis pathways, as observed for alanine (see below), and partly for branched chain amino acids.

Glyoxylate cycle The isocitrate lyase Icl1 was found in the cytosol and peroxisomes, but the next step of the glyoxylate pathway, malate synthase, was not clearly detected (Mls1 was below the cut-off and Dal7 never quantified). This suggest that the full glyoxylate cycle is not very active in the studied conditions. However, alternative reactions of glyoxylate exist, like alanine:glyoxylate aminotransferase (Agx1) and glyoxylate reductase (Gor1) found in the cytosol in both growth conditions. Remarkably, Gor1 was found in the mitochondria in *S. cerevisiae* (Reinders *et al.* 2006; Rintala *et al.* 2007), indicating different metabolic roles of glyoxylate and its converting enzymes in different yeasts.

Fermentation The unique K. *phaffii* pyruvate decarboxylase Pdc1 was found in the cytosol and in the peroxisomes in both tested growth conditions. Several alcohol dehydrogenases and aldehyde dehydrogenases were in the cytosol and peroxisomes (and partly in mitochondria). One is Adh2, identified by Karaoglan, Karaoglan and Inan (2015) as main alcohol dehydrogenase responsible for ethanol consumption in *K. phaffii* but named as Adh3, and further tested by Nocon *et al.* (2014). It is however difficult to allocate the metabolic function of those enzymes based on sequence similarities.

Methanol assimilation All enzymes involved in methanol assimilation were found in the peroxisomes (Russmayer *et al.* 2015), while methanol dissimilation is localized to the cytosol (van der Klei *et al.* 2006). The presence of those enzymes in the glucose-grown cells, in agreement with transcriptional regulation patterns (Gasser, Steiger and Mattanovich 2015), suggests a deregulation in the late glucose batch phase.

Gluconeogenesis All enzymes relevant for gluconeogenesis were found as expected in the cytosol. To mention are the isoenzymes of fructose bisphosphate aldolase, because the isoform Fba1–1, assumed to function in glycolysis and gluconeogenesis, was found in the cytosol, while Fba1–2 was localized in peroxisomes, where it obviously has an essential role in the xylulose-5-phosphate cycle for methanol assimilation (Russmayer *et al.* 2015).

Amino acid pathways

Amino acid synthesis Nearly all enzymes responsible for amino acid synthesis were found, although *K. phaffii* was grown on rich media. This is in agreement with Heyland *et al.* (2011) who showed that *de novo* synthesis of amino acids occurs in *K. phaffii* in both defined media supplemented with amino acids or in complex YPD medium. Most enzymes have the same localization as in *S. cerevisiae*, but still some remarkable differences were observed, like enzymes involved in alanine, aspartate, glutamate, branched-chain amino acid and lysine synthesis, which were not found in the mitochondria as expected. This was the case for the alanine aminotransferase Alt1, found in the peroxisomes, the two aspartate aminotransferases Aat1 and Aat2, found in peroxisomes and vacuole in glucose-grown cells, Aat2 also in the cytosol, both *K. phaffii* glutamate dehydrogenases Gdh2 and Gdh3 found in the cytosol and peroxisome and the glutamate synthase Glt1 found in the cytosol. In *S. cerevisiae*, branched-chain amino acid synthesis initiates in the mitochondria while the later steps are localized in the cytosol. Contrary, we found all *K. phaffii* related enzymes in the peroxisomes and/or cytosol, and few of the earlier steps' enzymes also in the mitochondria. In detail, no mitochondrial localization was found for Leu4 (in agreement with Förster *et al.* (2014)), and for Bat1. Along arginine synthesis, the ornithine carbamoyltransferase Arg3 was found in mitochondria, not in the cytosol. Regarding lysine synthesis, the homocitrate synthase Lys20 and Lys21, which are required for the first steps, localizes to peroxisomes and cytosol rather than to mitochondria, the next enzyme, the homoaconitase Lys4, was found in both peroxisomes and mitochondria, while all further enzymes were found in the cytosol, as in *S. cerevisiae*.

Amino acid transporter *Komagataella phaffii* has 38 genes with a putative role in amino acid transport at the plasma membrane or for intracellular transport. Only few plasma membrane permeases were found in the plasma membrane, and most were in the microsomes and Golgi, probably on the way to their final destination, or were never quantified. Some vacuolar permeases were found in the vacuole fraction. Regarding the mitochondria, additionally to the few known mitochondrial amino acids permeases, we found Avt1, in agreement with its predicted mitochondrial localization but in contrast to the vacuolar localization of the *S. cerevisiae* homolog.

Amino acid degradation Similar to *S. cerevisiae* (Dickinson, Salgado and Hewlins 2003), *K. phaffii* does not degrade all amino acids to metabolites, to be used as carbon and energy source. As noted above, amino acid transaminases are rather localized in the cytosol or peroxisomes than to mitochondria. After deamination, the Ehrlich pathway is available for e.g. branched chain and aromatic amino acids, however, the enzymes involved were never quantified, indicating that this pathway is silent at least in the analyzed growth conditions.

Nucleotide synthesis

All enzymes of *de novo* purine and pyrimidine synthesis were found as expected in the cytosol, except for the dihydroorotate dehydrogenase Ura1. As many other yeasts, *K. phaffii* has an oxygen-dependent mitochondrial enzyme, whereas an ancestor of the *Saccharomyces* lineage has acquired a cytosolic, oxygen-independent version of Ura1 during evolution of fermentative growth (Nagy, Lacroute and Thomas 1992; Dashko *et al.* 2014). Also the uridylate kinase Ura6 was found in the mitochondria, and not in the cytosol like the *S. cerevisiae* homolog. Our findings

are supported by the mitochondrial prediction of *K. phaffii* Ura6, as well as of the *Kluyveromyces lactis*, *C. albicans*, *Yarrowia lipolytica* and *O. parapolymorpha* homologs, and the cytosolic prediction of *S. cerevisiae* and *Schizosaccharomyces pombe Ura6*.

Beta-oxidation of fatty acids

As described by Russmayer *et al.* (2015), all proteins required for the metabolism of fatty acids in the course of beta-oxidation were found in the peroxisomes. Fox2 was also found in the microsomes, suggesting that in conditions of low or no beta-oxidation the key enzyme of beta-oxidation, might reside in the ER.

Lipid metabolism

Enzymes for lipid biosynthesis are well characterized and their subcellular localization is well described for *S. cerevisiae*, but only limited information are available for *K. phaffii*. Although similar localizations can be assumed, some exceptions might be expected. In general, biosynthesis of most lipids is associated to membrane associated organelles.

Phosphatidic acid Glycerol-3-phosphate-acyltransferases of *S. cerevisiae* are well described to localize to the ER and the plasma membrane. In contrast, we found both glycerol-3-phosphate-acyltransferases Sct1 and Gpt2 in microsomes and mitochondria, which are the major organelles for glycerophospholipid biosynthesis. The close proximity between those membranes that harbor lipid-synthesizing enzymes, might be required to establish a complete and continuous biosynthetic pathway.

Phospholipid biosynthesis Enzymes of the glycerophospholipid biosynthesis beyond the step of phosphatidic acid formation were scarcely found due to the sampling at mid/late exponential phase. Only two of those enzymes, which also show maximum activities in *S. cerevisiae* at the end of exponential growth (Janssen et *al.* 2000), were found. Regarding the phospholipid biosynthesis beyond the step of cytidine diphosphate diacylglycerol, only four proteins were found, three of which are required for phosphatidylcholin (PC) biosynthesis. Interestingly, we found PC biosynthetic enzymes of two alternative pathways, the Kennedy and the methylation pathway. Indeed, although in *S. cerevisiae* the methylation pathway is the major route of phosphatidylethanolamine and PC, the Kennedy pathway is also active (Gibellini and Smith 2010).

Non-polar lipid biosynthesis According to the fact that triacylglycerols (TAG) and only to lesser extent steryl esters (STE) are the major storage lipids in *K. phaffii*, only the major TAG synthase Lro1 (Ivashov *et al.* 2013b) and no STE synthases were found. Similarly to *S. cerevisiae*, Lro1 was found in the microsomes and mitochondria from glucose-grown cells and in microsomes and early Golgi from methanol-grown cells.

Sterol biosynthesis Similarly to *S. cerevisiae*, all proteins of the early sterol pathway were found in the cytosol, except Hmg1, which was found in the microsome as in *S. cerevisiae* but additionally in the mitochondria. This dual localization might be explained by co-purification of MAM fractions during mitochondria isolation (Vance 1990) as these membranous compartments are highly interconnected. The same dual localization was observed for many enzymes of the late sterol biosynthesis pathway, expected only in the ER. This might suggest that the supply of mature ergosterol to its final destination at the plasma membrane in *K. phaffii* involves interorganellar contact sites and is not mediated by a sterol gradient along the secretory route as in *S. cerevisiae* (Grillitsch *et al.* 2014). However, under methanol growth conditions all enzymes of late sterol biosynthetic enzymes were either only in the microsome or also in the Golgi.

Fatty acid import and activation *Komagataella phaffii* has only a reduced set of fatty acyl-CoA synthetases compared to *S. cerevisiae*. The only fatty acyl-CoA synthetase found in this study is Faa1, which is also the major acyl-CoA synthetase activity during exponential growth in *S. cerevisiae*.

Fatty acid biosynthesis Differently to *S. cerevisiae* which contains a cytosolic and a mitochondrial acetyl-CoA carboxylase required to start fatty acids biosynthesis, *K. phaffii* has only the cytosolic enzyme Acc1 co-localizing with the peroxisomes. Peroxisomal mis-localization of this enzyme, mediated by Pex5 despite the absence of peroxisomal targeting signal, is reported for cell culture after drug treatment (Jung *et al.* 2012). All subsequent steps in fatty acid *de novo* biosynthesis are conducted by the fatty acid synthases Fas1 and Fas2, found in the cytosol only in methanol-derived fractions but also in Golgi, vacuole and peroxisome from glucose- and methanol-derived fractions. This unexpected localization suggests the existence of a selective degradation pathway along the late secretory route to maintain cellular homeostasis and ensure their housekeeping functions.

Fatty acid elongation In *S. cerevisiae* fatty acid elongation takes place in the ER and is catalyzed by five enzymes. Although Elo3 is the major elongase of very long chain fatty acids, only Elo2 was found in the microsomes, whereas Elo3 and the putative very long fatty acid elongase Elo100, unique for *K. phaffii* and highly similar to Elo3, were in the mitochondria. Mitochondrial fatty acid elongation is considered a pathway of minor importance and only few reports are available in yeasts (Bessoule *et al.* 1987, Bessoule *et al.* 1988; Hiltunen *et al.* 2009). Moreover, mitochondria have different elongases, which were never quantified or below the cut-off. Mitochondrial membranes are mostly depleted of sphingolipids (lipid with very long chain fatty acids), suggesting that MAMs, which have a distinct proteome and are known to be involved in lipid metabolism (Raturi and Simmen 2013), might be the localization of those lipid-biosynthetic enzymes.

Fatty acid desaturases *Komagataella phaffii* has two isoforms of the Δ-9 fatty acid desaturase Ole1 and two additional desaturases Ode1 and Ode2, not present in *S. cerevisiae*. Except for the isoform Ole1–2, all those enzymes were found in the microsomes and in the Golgi.

Sphingolipids Yeast sphingolipid biosynthesis mainly takes place in the ER but is completed in the Golgi. Similarly to *S. cerevisiae*, there is a preferential microsomal localization of those enzymes, but slightly different co-localizations were observed depending on the carbon source.

Proteome atlas

To visualize the organelle proteomes and the subcellular localization of any protein of interest, data were implemented in an interactive map http://pichiagenome-ext.boku.ac.at/pp_protein_visualization/index10.html#. The map is based on a schematic view of the yeast cell (Fig. 6) and its organelles: the ER (perinuclear and cortical ER connected to each other by ER tubules), Golgi cisternae, plasma membrane, vacuole, peroxisome, cytosol and mitochondria. Organelles not analyzed in this study, i.e.

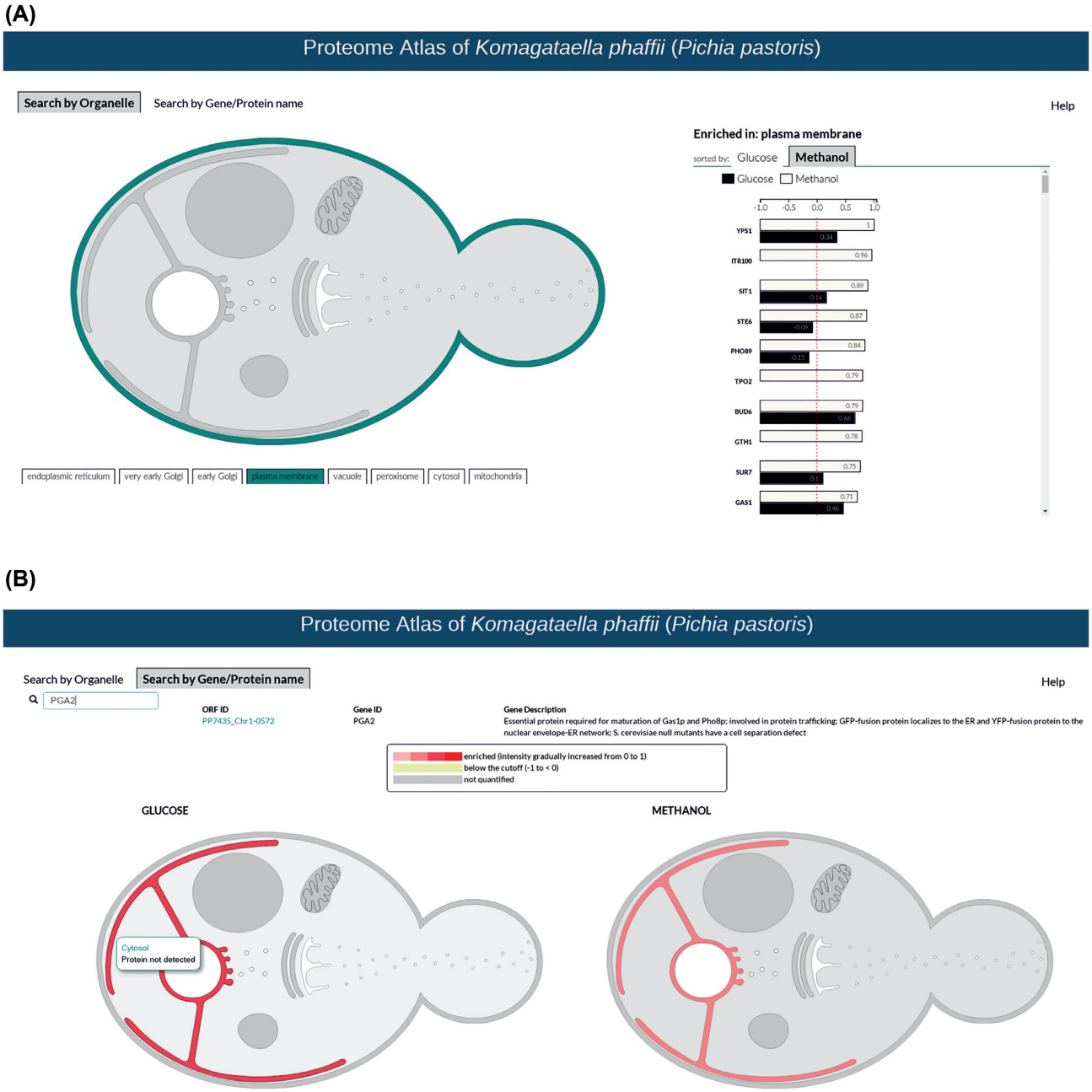

Figure 6. Proteome atlas of *K. phaffii*. **(A)**, Example of 'Search by Organelle': plasma membrane proteome in methanol-grown cells (proteins sorted by their enrichment). **(B)**, Example of 'Search by Gene/Protein name': Pga2 localization in glucose- and methanol-grown cells. The color code indicates if the protein was found enriched (red scale), below the cut-off (yellow) or never quantified (gray) in that organelle. Organelles not investigated in this study are marked in white.

nucleus, COPI and COPII vesicles, late Golgi and secretory vesicles are shown in white.

The option 'Search by Organelle' allows to get the proteome of an organelle of interest: proteins get listed sorted by their enrichment in the organelle isolated from glucose- (*per default*) or methanol-grown cells and a protein of interest can be searched in the selected compartment with the shortcut Strg + F (Fig. 6A). The option 'Search by Gene/Protein name' allows to search for a protein of interest by typing its gene name or ORF ID (Fig. 6B): the corresponding gene description (linked to www.pichiagenome.org) is shown and the organelles in which the protein was found enriched get red (with a color intensity directly proportional to the degree of enrichment), get yellow if the protein was found only below the cut-off and get gray if it was not quantified.

DISCUSSION

The compartmentalization of proteins and enzymes in organelles is a characteristic of eukaryotic cells. Compartment specific localization has evolved to carry out specific cellular processes and to enable the communication between organelles, which is important for cell maintenance, growth, function and response to external stimuli. Communication between organelles requires either direct contact between the

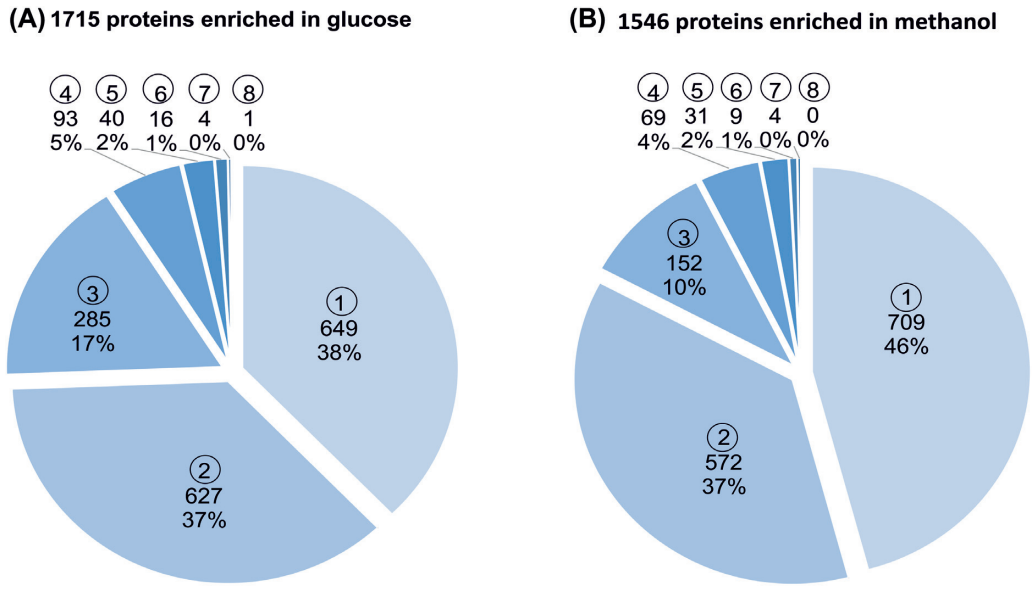

Figure 7. Specificity of protein enrichment. The pie charts illustrate, separately for **(A)**, glucose- and **(B)**, methanol-derived fractions, the number of proteins found enriched in a progressively increasing number of fractions (from a minimum of 1 to a maximum of 8). In each sector there is the number of enriched proteins, the corresponding percentage and, enclosed in circles, the number of fractions in which the proteins were enriched. The total number of proteins found to be enriched is also indicated on the upper part of the panels.

organelles or exchange of appropriate signals, like metabolites or ions. Besides that, proteins can have more than one final localization or be present in all cellular compartments that they have to pass to reach their final destination. Cell fractionation matched with mass spectrometry-based proteomics is a method of choice to study the subcellular localization of proteins, as applied in the present work. While contamination during cellular fractionation is possible, the results obtained show a very good specificity of the isolated organelles. Indeed, we show in this study that many proteins have a multiple final localization, which reflects the different biological functions which a protein can have in different cellular compartments. Alternative methods that avoid individual preparation of organelles, like e.g. hyperLOPIT (Christoforou *et al.* 2016; Nightingale *et al.* 2019), have the advantage to run all analyses from the same starting material, however, they will attribute each quantified protein to only one cellular compartment, so that the level of information on multiple localization would get lost.

All quantified proteins of each fraction were classified by their relative enrichment, leading to the identification of two partly overlapping Gaussian distributions for all fractions except for the peroxisomes. Combining three different criteria (localization of the *S. cerevisiae* homolog, localization prediction by WoLF PSORT and localization based on the suggested function (gene description)), we defined the most probable localization (efficiency on localization prediction of each single criterion is shown in Fig. S8, Supporting Information). Specific cut-offs were then applied to all organelles except the peroxisomes to separate, with a minimum false discovery rate, probable contaminants from likely positive hits which were then termed 'enriched' in the specific organelle. It should be noted that predictions were less specific for the plasma membrane, most probably because of the inefficient WoLF PSORT prediction of plasma membrane proteins.

Indeed, 74% and 83% of proteins from glucose- and methanol-grown cells, respectively, were enriched in one or maximum two fractions, and the percentage of proteins enriched in higher numbers of fractions progressively drops toward zero (Fig. 7A and B). Although the carbon source did not have a severe effect on the specificity of protein enrichment, a slightly higher specificity was observed for samples derived from methanol-grown cells. The higher percentage of proteins enriched in one unique fraction in methanol derived samples is shown in Fig. 7. No large differences in the organelle specific proteomes were observed comparing glucose- to methanol-grown cells. We found 152 glucose-specific hits (proteins enriched only in glucose-derived fractions but never quantified in methanol), mainly related to transcription, RNA processing and nucleus and 60 methanol-specific hits (proteins enriched only in methanol-derived fractions but never quantified in glucose), which were mainly ER and vacuole-related proteins (Fig. 8).

The organelle proteomes provided in this work reflect the knowledge of the *S. cerevisiae* proteome and of few published data on *K. phaffii*, but also point at differences and unexpected localizations. Comparison of the two yeasts showed indeed that only 159 proteins have been explicitly found in a different organelle (Fig. 5). However, only for approximately 20% of these proteins the experimental result in *K. phaffii* is supported by the predicted localization based on computational analysis of the *K. phaffii* proteome. A closer look at the proteome of each organelle allowed to highlight some organelle specific differences. For example, we found many vacuolar and plasma membrane transporters in intermediate organelles but never quantified at the expected destination. Plasma membranes have more transport proteins in methanol-grown cells, suggesting that on a less favorable carbon source the cells get prepared for the uptake of more different nutrients. Nearly all predicted vacuolar proteins were found in the vacuole fraction, and the most enriched ones, mainly vacuolar proteins, were the same between glucose- and methanol-grown cells, indicating the high quality of fraction preparations. Furthermore, there is an unusually high number of

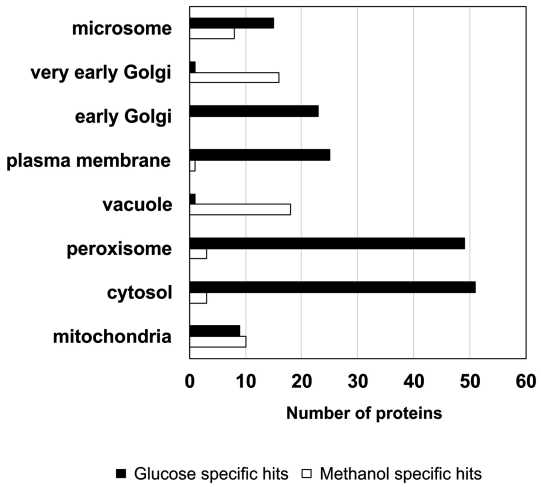

Figure 8. Carbon source specific protein hits. For each fraction the glucose specific hits (proteins specifically enriched only in glucose-derived fractions and never quantified in methanol-derived fractions; black bars) and the methanol specific hits (proteins specifically enriched only in methanol-derived fractions and never quantified in glucose-derived fractions; white bars) are shown.

proteins with unknown function localized in the *K. phaffii* vacuole, the majority thereof confirming the vacuolar localization described for their putative homolog in *S. cerevisiae* (Wiederhold *et al.* 2009).

Most enzymes of the central carbon metabolism were found with just few differences to their localization in *S. cerevisiae*. As we have shown previously (Russmayer *et al.* 2015), isoforms of several enzymes of the methanol assimilation pathway were found in the peroxisomes of methanol-grown cells. Different to *S. cerevisiae*, all TCA cycle enzymes were also found in the peroxisomes, indicating that in *K. phaffii* the entire TCA cycle may also be active in the peroxisomes. The absence of paralogs of TCA enzymes may underlay a mechanism of dual localization. Malic enzyme was only found in the peroxisomes and the cytosol, while in *S. cerevisiae* it refills the pyruvate pool for mitochondrial amino acid synthesis. Correspondingly, several enzymes of amino acid synthesis were found in the peroxisomes or cytosol, rather than in mitochondria, as in *S. cerevisiae*. The pathways discussed here and the localization of the corresponding enzymes will be an important resource for refining the metabolic models of *K. phaffii* (Tomas-Gamisans, Ferrer and Albiol 2018), and for metabolic engineering to produce biochemicals with this yeast (Pena *et al.* 2018).

Refining of the annotation of protein isoforms can take advantage of the specific organelle localization. As described by Russmayer *et al.* (2015), isoforms of a defined protein might have different localization and an organelle-specific function, and further examples of isoforms with different localization were also faced in this study. On the other hand, *K. phaffii* often lacks paralogs, which are present in *S. cerevisiae* due to genome duplication during its evolution. While it is often difficult to annotate the correct isoform by sequence similarity, based on this subcellular proteomics data we can now more easily identify the functional *S. cerevisiae* homolog.

As previously reported, 27% of *K. phaffii* ORFs are not yet annotated (Valli *et al.* 2016), similarly to the 21% not characterized or dubious ORFs in *S. cerevisiae* (SGD Genome Inventory by July 2019 http://www.yeastgenome.org/genomesnapshot). In the present work, we quantified 220 unknown proteins, 128 of which having interesting patterns (Supporting Information File 6). Some were among the most enriched proteins for certain organelles, some were organelle-specific and some carbon source-specific. The experimental verification of their localization, which correlated with the predicted localization and the putative function assigned by sequence homology or the presence of conserved domains, will help to elucidate the true cellular functions of these unknown proteins in future.

Finally, we introduce an interactive map of the organelle specific proteomes of *K. phaffii* (Proteome atlas of *K. phaffii*), based on the quantitative MS data, to visualize the proteomes of the studied organelles as well as the subcellular localization of any protein of interest.

DATA AVAILABILITY

The mass spectrometry proteomics data have been deposited to the ProteomeXchange Consortium via the PRIDE (Vizcaino *et al.* 2016) partner repository with the data set identifier PXD011220.

SUPPLEMENTARY DATA

Supplementary data are available at *FEMSYR* online.

ACKNOWLEDGMENTS

This work has been supported by the Federal Ministry for Digital and Economic Affairs (bmwd), the Federal Ministry for Transport, Innovation and Technology (bmvit), the Styrian Business Promotion Agency SFG, the Standortagentur Tirol, Government of Lower Austria and ZIT—Technology Agency of the City of Vienna through the COMET-Funding Program managed by the Austrian Research Promotion Agency FFG. EQ BOKU VIBT GmbH is acknowledged for providing mass spectrometry equipment. LK and VI were financed by the Translational Research Programme of the Austrian Science Fund (FWF), project *Pichia* Lipidomics, TRP9, awarded to GD. NT was supported by the Christian Doppler Research Association (Christian Doppler Laboratory for Innovative Immunotherapeutics), Merck KGaA, as well as the Austrian Science Fund (FWF W1224—Doctoral Program on Biomolecular Technology of Proteins—BioToP). We would like to thank Ralf Erdmann (Systems Biochemistry, Institute of Biochemistry and Pathobiochemistry, Faculty of Medicine, Ruhr-Universität Bochum, 44801 Bochum, Germany) for providing antisera against the peroxisomal membrane protein Pex3 and Howard Riezman (Department of Biochemistry, NCCR Chemical Biology, University of Geneva, Geneva, Switzerland) for providing antisera against the integral Golgi protein Emp47. We would like to thank Anton Glieder (Institute of Molecular Biotechnology, Graz University of Technology, Austria) for providing the strain CBS7435*Ku70 his4* and the plasmid pGAPzA-eGFP and Benjamin Glick (Department of Molecular Genetics and Cell Biology, University of Chicago, Illinois) for providing the strain PPY12 carrying the plasmid GAP-GFP-GOS1.

Conflicts of interest. None declared.

REFERENCES

Agrawal G, Subramani S. De novo peroxisome biogenesis: evolving concepts and conundrums. *Biochim Biophys Acta* 2016;**1863**:892–901.

Bessoule JJ, Lessire R, Rigoulet M *et al.* Fatty acid synthesis in mitochondria from *Saccharomyces cerevisiae*. *FEBS Lett* 1987;**214**:158–62.

Bessoule JJ, Lessire R, Rigoulet M *et al*. Localization of the synthesis of very-long-chain fatty acid in mitochondria from *Saccharomyces cerevisiae*. *Eur J Biochem* 1988;**177**:207–11.

Bevis BJ, Hammond AT, Reinke CA *et al*. De novo formation of transitional ER sites and Golgi structures in *Pichia pastoris*. *Nat Cell Biol* 2002;**4**, 750–6.

Boles E, de Jong-Gubbels P, Pronk JT. Identification and characterization of MAE1, the *Saccharomyces cerevisiae* structural gene encoding mitochondrial malic enzyme. *J Bacteriol* 1998;**180**:2875–82.

Brandina I, Graham J, Lemaitre-Guillier C *et al*. Enolase takes part in a macromolecular complex associated to mitochondria in yeast. *Biochim Biophys Acta* 2006;**1757**:1217–28.

Bridges HR, Fearnley IM, Hirst J. The subunit composition of mitochondrial NADH:ubiquinone oxidoreductase (complex I) from *Pichia pastoris*. *Mol Cell Proteomics* 2010;**9**: 2318–26.

Christoforou A, Mulvey CM, Breckels LM *et al*. A draft map of the mouse pluripotent stem cell spatial proteome. *Nat Commun* 2016;**7**:8992.

Cohen Y, Klug YA, Dimitrov L *et al*. Peroxisomes are juxtaposed to strategic sites on mitochondria. *Mol Biosyst* 2014;**10**:1742–8.

Dashko S, Zhou N, Compagno C *et al*. Why, when, and how did yeast evolve alcoholic fermentation? *FEMS Yeast Res* 2014;**14**:826–32.

Dean N. Asparagine-linked glycosylation in the yeast Golgi. *Biochim Biophys Acta* 1999;**1426**:309–22.

Delic M, Valli M, Graf AB *et al*. The secretory pathway: exploring yeast diversity. *FEMS Microbiol Rev* 2013;**37**:872–914.

Dickinson JR, Salgado LE, Hewlins MJ. The catabolism of amino acids to long chain and complex alcohols in *Saccharomyces cerevisiae*. *J Biol Chem* 2003;**278**:8028–34.

Fraley C, Raftery AE. Model-Based clustering, discriminant analysis, and density estimation. *J Am Statist Assoc* 2002;**97**:611–31.

Fraley C, Raftery AE, Murphy TB *et al*. mclust Version 4 for R: Normal mixture modeling for model-based clustering, classification, and density estimation. 2012.

Förster J, Famili I, Fu P *et al*. Genome-scale reconstruction of the *Saccharomyces cerevisiae* metabolic network. *Genome Res* 2003;**13**:244–53.

Förster J, Halbfeld C, Zimmermann M *et al*. A blueprint of the amino acid biosynthesis network of hemiascomycetes. *FEMS Yeast Res* 2014;**14**:1090–100.

Gabaldon T, Snel B, van Zimmeren F *et al*. Origin and evolution of the peroxisomal proteome. *Biol Direct* 2006;**1**:8.

Gaigg B, Simbeni R, Hrastnik C *et al*. Characterization of a microsomal subfraction associated with mitochondria of the yeast, *Saccharomyces cerevisiae*. Involvement in synthesis and import of phospholipids into mitochondria. *Biochim Biophys Acta* 1995;**1234**:214–20.

Gasser B, Steiger MG, Mattanovich D. Methanol regulated yeast promoters: production vehicles and toolbox for synthetic biology. *Microb Cell Fact* 2015;**14**:196.

Gibellini F, Smith TK. The Kennedy pathway–De novo synthesis of phosphatidylethanolamine and phosphatidylcholine. *IUBMB Life* 2010;**62**:414–28.

Grillitsch K, Tarazona P, Klug L *et al*. Isolation and characterization of the plasma membrane from the yeast *Pichia pastoris*. *Biochim Biophys Acta* 2014;**1838**:1889–97.

Haid A, Suissa M. Immunochemical identification of membrane proteins after sodium dodecyl sulfate-polyacrylamide gel electrophoresis. *Methods Enzymol* 1983;**96**:192–205.

Hamilton SR, Bobrowicz P, Bobrowicz B *et al*. Production of complex human glycoproteins in yeast. *Science* 2003;**301**:1244–6.

Herzig S, Raemy E, Montessuit S *et al*. Identification and functional expression of the mitochondrial pyruvate carrier. *Science* 2012;**337**:93–96.

Heyland J, Fu J, Blank LM *et al*. Carbon metabolism limits recombinant protein production in *Pichia pastoris*. *Biotechnol Bioeng* 2011;**108**, 1942–53.

Hiltunen JK, Schonauer MS, Autio KJ *et al*. Mitochondrial fatty acid synthesis type II: more than just fatty acids. *J Biol Chem* 2009;**284**:9011–5.

Huh WK, Falvo JV, Gerke LC *et al*. Global analysis of protein localization in budding yeast. *Nature* 2003;**425**:686–91.

Ivashov VA, Grillitsch K, Koefeler H *et al*. Lipidome and proteome of lipid droplets from the methylotrophic yeast *Pichia pastoris*. *Biochim Biophys Acta* 2013a;**1831**:282–90.

Ivashov VA, Zellnig G, Grillitsch K *et al*. Identification of triacylglycerol and steryl ester synthases of the methylotrophic yeast *Pichia pastoris*. *Biochim Biophys Acta* 2013b;**1831**:1158–66.

Janssen MJ, Koorengevel MC, de Kruijff B *et al*. The phosphatidylcholine to phosphatidylethanolamine ratio of *Saccharomyces cerevisiae* varies with the growth phase. *Yeast* 2000;**16**:641–50.

Johnson MA, Waterham HR, Ksheminska GP *et al*. Positive selection of novel peroxisome biogenesis-defective mutants of the yeast *Pichia pastoris*. *Genetics* 1999;**151**:1379–91.

Jung D, Abu-Elheiga L, Ayuzawa R *et al*. Mislocalization and inhibition of acetyl-CoA carboxylase 1 by a synthetic small molecule. *Biochem J* 2012;**448**: 409–16.

Just WW, Peranen J. Small GTPases in peroxisome dynamics. *Biochim Biophys Acta* 2016;**1863**:1006–13.

Karaoglan M, Karaoglan FE, Inan M. Functional analysis of alcohol dehydrogenase (ADH) genes in *Pichia pastoris*. *Biotechnol Lett* 2015;**38**:463–9

Karhinen L, Makarow M. Activity of recycling Golgi mannosyltransferases in the yeast endoplasmic reticulum. *J Cell Sci* 2004;**117**:351–8.

Klug L, Tarazona P, Gruber C *et al*. The lipidome and proteome of microsomes from the methylotrophic yeast *Pichia pastoris*. *Biochim Biophys Acta* 2014;**1841**:215–26.

Laemmli UK. Cleavage of structural proteins during the assembly of the head of bacteriophage T4. *Nature* 1970;**227**:680–5.

Lowry OH, Rosebrough NJ, Farr AL *et al*. Protein measurement with the Folin phenol reagent. *J Biol Chem* 1951;**193**:265–75.

Lu H, Li F, Sánchez BJ *et al*. A consensus *S. cerevisiae* metabolic model Yeast8 and its ecosystem for comprehensively probing cellular metabolism. *Nat Commun* 2019;**10**:3586.

Maccani A, Landes N, Stadlmayr G *et al*. *Pichia pastoris* secretes recombinant proteins less efficiently than Chinese hamster ovary cells but allows higher space-time yields for less complex proteins. *Biotechnol J* 2014;**9**:526–37.

Marsalek L, Gruber C, Altmann F *et al*. Disruption of genes involved in CORVET complex leads to enhanced secretion of heterologous carboxylesterase only in protease deficient *Pichia pastoris*. *Biotechnol J*. 2017;**12**. doi: 10.1002/biot.201600584.

Mattanovich D, Sauer M, Gasser B. Industrial microorganisms: *Pichia pastoris*. In: Wittmann C, Liao JC . (eds). *Industrial Biotechnology: Microorganisms*. Weinheim, DE: Wiley-VCH Verlag GmbH & Co. KGaA, 2017;**1**:687–714.

Murley A, Nunnari J. The emerging network of mitochondria-organelle contacts. *Mol Cell* 2016;**61**:648–53.

Nagy M, Lacroute F, Thomas D. Divergent evolution of pyrimidine biosynthesis between anaerobic and aerobic yeasts. *Proc Natl Acad Sci U S A* 1992;**89**:8966–70.

Nightingale DJ, Geladaki A, Breckels LM *et al*. The subcellular organisation of *Saccharomyces cerevisiae*. *Curr Opin Chem Biol* 2019;**48**:86–95.

Nocon J, Steiger MG, Pfeffer M *et al*. Model based engineering of *Pichia pastoris* central metabolism enhances recombinant protein production. *Metab Eng* 2014;**24**:129–38.

Ohsumi Y, Anraku Y. Active transport of basic amino acids driven by a proton motive force in vacuolar membrane vesicles of *Saccharomyces cerevisiae*. *J Biol Chem* 1981;**256**:2079–82.

Pena DA, Gasser B, Zanghellini J *et al*. Metabolic engineering of *Pichia pastoris*. *Metab Eng* 2018;**50**:2–15.

Pichler P, Kocher T, Holzmann J *et al*. Peptide labeling with isobaric tags yields higher identification rates using iTRAQ 4-plex compared to TMT 6-plex and iTRAQ 8-plex on LTQ Orbitrap. *Anal Chem* 2010;**82**:6549–58.

Polupanov AS, Nazarko VY, Sibirny AA. CCZ1, MON1 and YPT7 genes are involved in pexophagy, the Cvt pathway and non-specific macroautophagy in the methylotrophic yeast *Pichia pastoris*. *Cell Biol Int* 2011;**35**:311–9.

Powers D. Evaluation: From Precision, Recall and F-Measure to ROC, Informedness, Markedness & Correlation. *Journal of Machine Learning Technologies* 2011;**2**:37–63.

Prielhofer R, Maurer M, Klein J *et al*. Induction without methanol: novel regulated promoters enable high-level expression in *Pichia pastoris*. *Microb Cell Fact* 2013;**12**:5.

Puxbaum V, Mattanovich D, Gasser B. Quo vadis? The challenges of recombinant protein folding and secretion in *Pichia pastoris*. *Appl Microbiol Biotechnol* 2015;**99**:2925–38.

R CoreTeam. *R: A Language and Environment for Statistical Computing*. Vienna, Austria: R Foundation for Statistical Computing, 2017 https://www.R-project.org/.

Raturi A, Simmen T. Where the endoplasmic reticulum and the mitochondrion tie the knot: the mitochondria-associated membrane (MAM). *Biochim Biophys Acta* 2013;**1833**:213–24.

Rebnegger C, Graf AB, Valli M *et al*. In *Pichia pastoris*, growth rate regulates protein synthesis and secretion, mating and stress response. *Biotechnol J* 2014;**9**:511–25.

Reinders J, Zahedi RP, Pfanner N *et al*. Toward the complete yeast mitochondrial proteome: multidimensional separation techniques for mitochondrial proteomics. *J Proteome Res* 2006;**5**:1543–54.

Rintala E, Pitkanen JP, Vehkomaki ML *et al*. The ORF YNL274c (GOR1) codes for glyoxylate reductase in *Saccharomyces cerevisiae*. *Yeast* 2007;**24**:129–36.

Russmayer H, Buchetics M, Gruber C *et al*. Systems-level organization of yeast methylotrophic lifestyle. *BMC Biol* 2015;**13**:80.

Sarry JE, Chen S, Collum RP *et al*. Analysis of the vacuolar luminal proteome of *Saccharomyces cerevisiae*. *FEBS J* 2007;**274**:4287–305.

Schollenberger L, Gronemeyer T, Huber CM *et al*. RhoA regulates peroxisome association to microtubules and the actin cytoskeleton. *PLoS One* 2010;**5**:e13886.

Shen XX, Opulente DA, Kominek J *et al*. Tempo and mode of genome evolution in the budding yeast subphylum. *Cell* 2018;**175**:1533–45.

Tamura N, Oku M, Sakai Y. Atg8 regulates vacuolar membrane dynamics in a lipidation-independent manner in *Pichia pastoris*. *J Cell Sci* 2010;**123**:4107–16.

Tomas-Gamisans M, Ferrer P, Albiol J. Fine-tuning the P. pastoris iMT1026 genome-scale metabolic model for improved prediction of growth on methanol or glycerol as sole carbon sources. *Microb Biotechnol* 2018;**11**:224–37.

Urbanowski JL, Piper RC. The iron transporter Fth1p forms a complex with the Fet5 iron oxidase and resides on the vacuolar membrane. *J Biol Chem* 1999;**274**:38061–70.

Valli M, Tatto NE, Peymann A *et al*. Curation of the genome annotation of *Pichia pastoris* (*Komagataella phaffii*) CBS7435 from gene level to protein function. *FEMS Yeast Res* 2016;**16**:fow051.

van der Klei IJ, Yurimoto H, Sakai Y *et al*. The significance of peroxisomes in methanol metabolism in methylotrophic yeast. *Biochim Biophys Acta* 2006;**1763**:1453–62.

Vance JE. Phospholipid synthesis in a membrane fraction associated with mitochondria. *J Biol Chem* 1990;**265**:7248–56.

Vervecken W, Kaigorodov V, Callewaert N *et al*. In vivo synthesis of mammalian-like, hybrid-type N-glycans in *Pichia pastoris*. *Appl Environ Microbiol* 2004;**70**:2639–46.

Vizcaino JA, Csordas A, del-Toro N *et al*. 2016 update of the PRIDE database and its related tools. *Nucleic Acids Res* 2016;**44**:D447–56.

Wang W, Subramani S. Assays to monitor pexophagy in Yeast. *Methods Enzymol* 2017;**588**:413–27.

Wiederhold E, Gandhi T, Permentier HP *et al*. The yeast vacuolar membrane proteome. *Mol Cell Proteomics* 2009;**8**:380–92.

Wiederhold E, Veenhoff LM, Poolman B *et al*. Proteomics of *Saccharomyces cerevisiae* Organelles. *Mol Cell Proteomics* 2010;**9**:431–45.

Wojtera-Kwiczor J, Groß F, Leffers HM *et al*. Transfer of a Redox-Signal through the Cytosol by Redox-Dependent Microcompartmentation of Glycolytic Enzymes at Mitochondria and Actin Cytoskeleton. *Front Plant Sci* 2013;**3**:284.

Wriessnegger T, Gübitz G, Leitner E *et al*. Lipid composition of peroxisomes from the yeast *Pichia pastoris* grown on different carbon sources. *Biochim Biophys Acta* 2007;**1771**:455–61.

Wriessnegger T, Leitner E, Belegratis MR *et al*. Lipid analysis of mitochondrial membranes from the yeast *Pichia pastoris*. *Biochim Biophys Acta* 2009;**1791**:166–72.

Yamashita SI, Oku M, Sakai Y *et al*. Experimental systems to study yeast pexophagy. *Methods Mol Biol* 2017;**1595**:249–55.